Uncorrected Proof

Journal of
Water & Climate Change

Journal of Water and Climate Change Vol 00 No 0, 1 doi: 10.2166/wcc.2024.492

Impact of climate change on the streamflow in northern Patagonia

Juan Rivera [a,*], Malaëka Robo[b], Emilio Bianchi[c] and Cristóbal Mulleady[d]

[a] Consejo Nacional de Investigaciones Científicas y Técnicas (CONICET) - Instituto Argentino de Nivología, Glaciología y Ciencias Ambientales (CCT-Mendoza/CONICET), Av. Ruiz Leal s/n, Parque General San Martín, 5500 Mendoza, Argentina
[b] National School of Meteorology (ENM), 42 avenue Gaspard Coriolis, 31057 Toulouse, France
[c] Consejo Nacional de Investigaciones Científicas y Técnicas (CONICET), Universidad Nacional de Río Negro (UNRN), Anasagasti 1463, 8400 San Carlos de Bariloche, Argentina
[d] Comisión Nacional de Energía Atómica (CNEA), Centro Atómico Bariloche, Av. Bustillo 9500, 8400 San Carlos de Bariloche, Argentina
*Corresponding author. E-mail: jrivera@mendoza-conicet.gob.ar

JR, 0000-0001-7754-1612

ABSTRACT

Streamflow simulations from the Inter-Sectoral Impact Model Intercomparison Project phase 2b (ISIMIP2b) were analyzed to evaluate future changes in surface water resources over northern Patagonia, a region that contributes significantly to the total hydropower production of Argentina. Ten global hydrological models (GHMs), forced by four general circulation models, effectively capture the winter streamflow maximum in the Negro river basin. However, most of them face challenges in simulating the late-spring pulse due to a misrepresentation of temperature over the higher elevations of the Andes. We quantified the future streamflow evolution using a multi-model ensemble from a subset of the best-performing GHMs under the RCP2.6 and RCP6.0 emission scenarios for two temporal horizons. According to the multi-model ensemble, there is a projected decrease in the annual streamflow of the analyzed rivers, which is more important considering the RCP6.0 scenario during the late 21st century, reaching up to −40% relative to the 1979–2005 reference period. This reduction is attributed to the projected precipitation decline in the headwaters of the Negro river basin in response to changes in the surface pressure patterns. These results have implications for regional water authorities for the development of adaptation plans considering future demand projections.

Key words: climate change, future projections, global hydrological models, Patagonia, streamflow

HIGHLIGHTS

- A set of global hydrological models (GHMs) from the ISIMIP2b project was used to characterize streamflow changes in the Comahue region.
- A decrease in the annual streamflow is projected along the 21st century, particularly for the Neuquén river.
- Uncertainty is mainly linked to the global climate models used to drive the GHMs.
- Hydropower generation and irrigation for agriculture are expected to face future reductions.

GRAPHICAL ABSTRACT

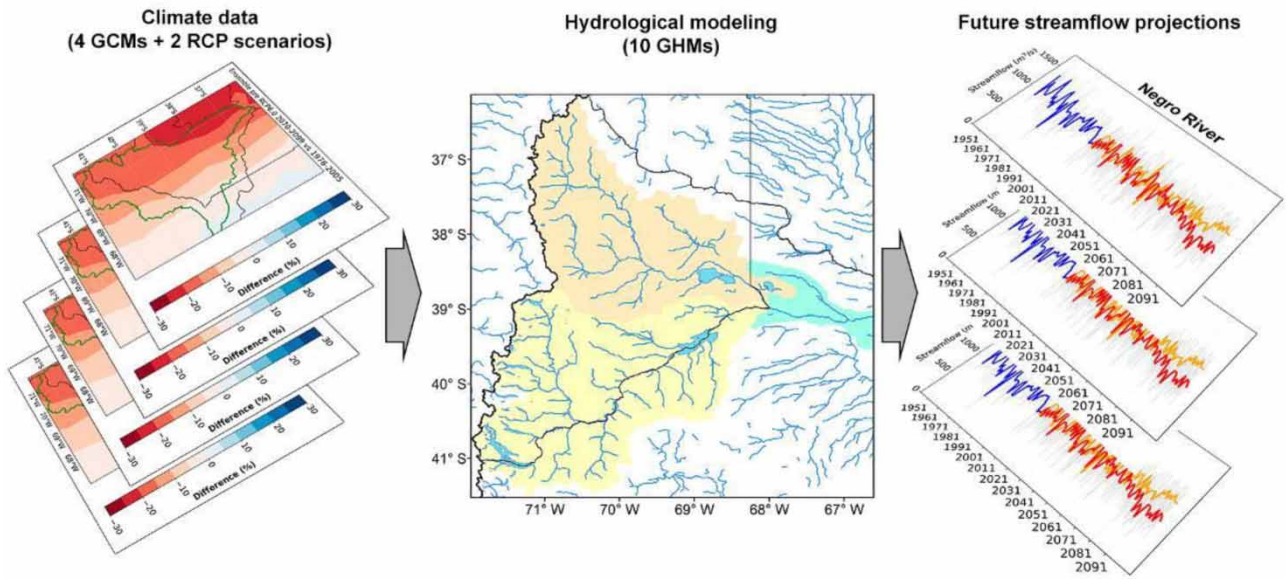

1. INTRODUCTION

Water resources availability is strongly affected by climate change. According to the last report of the Intergovernmental Panel on Climate Change (IPCC), the global water cycle exhibited an overall strengthening since at least 1980 (Gulev *et al.* 2021). This strengthening was attributed to human influences affecting the global energy budget, such as the increased concentrations of greenhouse gases. Human-induced climate change has significant implications for changes in atmospheric circulation, resulting in substantial changes in precipitation patterns, albeit with regional heterogeneity in trend patterns. The changes in the spatial and temporal patterns of precipitation and evaporation rates have caused variations in streamflow in major rivers of the world (Dai *et al.* 2009; Zhang *et al.* 2023). Moreover, the increase in global temperatures has led to significant changes in the hydrological cycle components associated to the cryosphere, including reductions in snow cover, snow depth, and glacier volume, together with an early snowmelt pulse (Huss *et al.* 2017; Shannon *et al.* 2019).

The main rivers in the northern region of Argentine Patagonia, known as the Comahue region, originate in the Andes Ranges within the latitudinal band between 37° and 41°S. The streamflow in these rivers is controlled by variations in winter precipitation, snowmelt, and glaciermelt (Vich *et al.* 2014). The main socio-economic activities in the northern Patagonia region directly rely on the water availability of the Limay, Neuquén, and Negro rivers (Raggio & Saurral 2021). Up to 25% of the hydropower production of Argentina is generated by hydropower plants such as El Chocón and Piedra del Águila, located on the Limay river, and the Cerros Colorados Complex, located on the Neuquén river, amounting to approximately USD300 million per year (Seoane & López 2007; Romero *et al.* 2020; González *et al.* 2023). Irrigation for agricultural production, oil and mining exploitation, tourism, and sport fishing, also depend on the available water resources (Pessacg *et al.* 2020). For instance, intensive agriculture in the High Valley (Alto Valle) along the Negro river accounts for more than 75% of the total national production of apples and pears (Brendel *et al.* 2020).

Due to the socio-economic relevance of regional water availability, several studies have focused on developing statistical precipitation forecasts over northern Patagonia, particularly for the austral winter months (González *et al.* 2010; Romero *et al.* 2020). These seasonal forecasts are linked to streamflow generation and enable decision-makers to optimize the operation of dams and irrigation channels. Nevertheless, water authorities face not only fluctuations in precipitation occurring on seasonal or interannual timescales but also long-term changes that pose a threat to water security. For instance, a declining long-term trend in precipitation and streamflow over northern Patagonia has been identified (Seoane & López 2007; Lauro *et al.* 2019; Brendel et al. 2020), particularly for minimum annual streamflow, leading to an increase in the frequency of hydrological droughts (Rivera *et al.* 2018). This decreasing trend over the last century has been attributed to changes in large-scale circulation patterns, such as the poleward expansion of the Hadley Circulation and the consequent displacement

of the extratropical storm tracks (Rivera *et al.* 2020). Part of this expansion mechanism, which modifies hemispheric circulation patterns, can be explained by the increase in greenhouse gas concentrations (Mindlin *et al.* 2020; Villamayor *et al.* 2021). Henceforth, the influence of anthropogenic climate change on the modulation of regional streamflow and, thus, water availability is of substantial significance.

Future changes in the magnitude, variability, and temporal distribution of streamflow are dependent mainly on the projected patterns of temperature, precipitation amount, phase, and timing. Considering the future climate projections for northern Patagonia, it is expected a significant reduction of precipitation over the headwaters of the main rivers in the region, particularly during the cold months (Almazroui *et al.* 2021; Raggio & Saurral 2021). Projected temperature increases are robust even under low-emissions scenarios (Almazroui *et al.* 2021), compromising water reservoirs associated with glaciers and permafrost (Forni *et al.* 2018; Hock *et al.* 2019). The expected changes in temperature and precipitation will increase the frequency and severity of droughts, especially under the more severe emissions scenarios (Spinoni *et al.* 2020), with a direct impact on streamflow generation. Irrigated agriculture, hydropower generation, and water supply for urban and rural populations will undoubtedly be affected by projected streamflow reductions. In this context, quantifying the expected changes in regional streamflow over the 21st century is of paramount importance for understanding and anticipating potential water stress episodes and developing policy measures to adapt to these changes.

Few studies have assessed the impacts of future climate change on streamflow in northern Patagonia region. These studies commonly used a complex modeling chain, starting with bias-corrected statistically downscaled general circulation model (GCM) projections of future climate to drive hydrological models to produce future streamflow projections (Krysanova *et al.* 2018; Miller *et al.* 2021). An early study from Seoane & López (2007) estimated a projected streamflow reduction for the Limay river of nearly 10% by the end of the 21st century. However, more recent evaluations projected a reduction ranging from 20% (Pessacg *et al.* 2020) to 50% (Raggio & Saurral 2021), depending on the selected GCMs, hydrological models, and rivers. These studies underscore large uncertainties in future streamflow projections for northern Patagonia, and call for new evaluations to account for climate change impacts on regional water resources.

A valuable dataset to perform this kind of research is based on streamflow simulations from global hydrological models (GHMs) belonging to the Inter-Sectoral Impact Model Intercomparison Project (ISIMIP). These simulations were commonly used to quantify the impact of climate change on water resources, addressing aspects such as the seasonal dynamics of river streamflow, the mean annual discharge and the frequency and intensity of streamflow extremes from both regional and global perspectives (Gosling *et al.* 2017; Krysanova *et al.* 2017; Zaherpour *et al.* 2018). For example, Ju *et al.* (2023) used a multi-model ensemble based on six GHMs to evaluate the uncertainty in terrestrial water storage projections at global scale. Using a similar methodological approach, Asadieh & Krakauer (2017) identified global changes in high and low streamflow extremes over the 21st century.

The objective of this research is to use the GHM simulations from ISIMIP to assess future changes in the streamflow of the main rivers in northern Patagonia (Limay, Neuquén, and Negro rivers). The GHMs are driven by multiple GCMs forced under two Representative Concentration Pathways (RCPs) that provide quantitative descriptions of greenhouse gases evolution throughout the 21st century. Based on GHM validation over the historical period and using a multi-model ensemble approach with the best GHMs, we aim to quantify the projected changes in surface water resources and assess their uncertainty. The structure of the paper is organized as follows: Section 2 describes the study area and data; Section 3 summarizes the methods used in the evaluation; Section 4 provides the main results obtained in the model validation, the future streamflow projections and its main drivers; the discussion of the main outcomes is included in Section 5; while the conclusions are summarized in Section 6.

2. DATA AND STUDY AREA

2.1. Study area

The northern region of Argentine Patagonia is located roughly between 37° and 41°S, bounded by the Andes ranges in the west and the steppe in the east (Figure 1(a)). The complex topography of the Andes alters the spatial patterns of temperature and precipitation across the region. The mean elevation of the Andes gradually decreases from over 3,000 m around 37°S to 1,500 m south of 41°S. This factor shapes the mean annual temperature climatology, with temperatures lower than 8 °C over the higher elevations, increasing to more than 12 °C toward the east (Figure 1(b)). Due to the prevailing westerly winds at these latitudes, the Andes capture the passages of moist air masses from the Pacific Ocean, creating a precipitation maximum

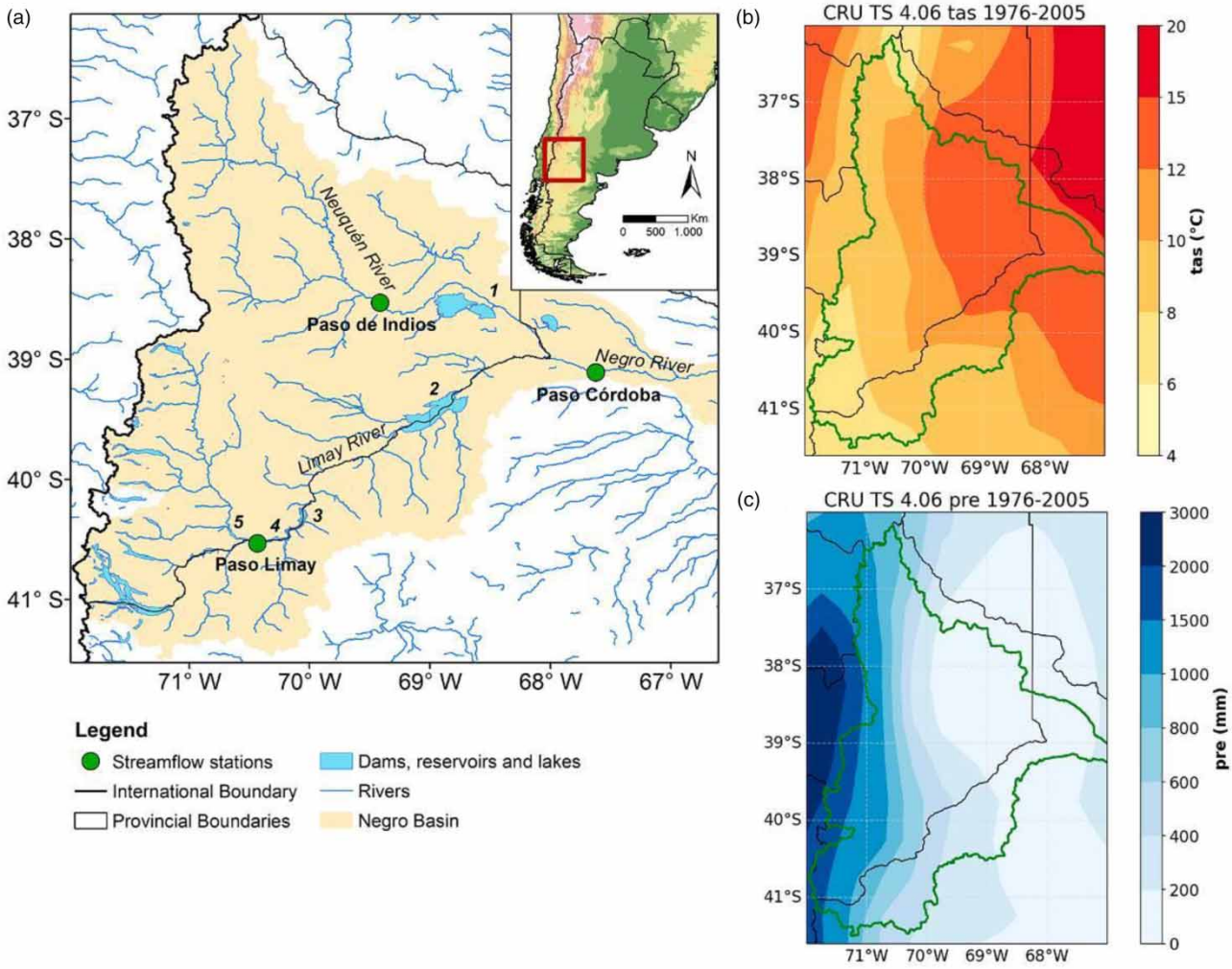

Figure 1 | Location of the study area showing (a) the Negro River Basin with the main rivers of northern Patagonia, the location of the gauging stations at each of the rivers, and the main reservoirs (1 – Cerros Colorados Complex; 2 – El Chocón; 3 – Alicurá; 4 – Piedra del Águila; 5 – Pichi Picún Leufú); (b) the spatial pattern of mean annual temperature and (c) mean annual precipitation for the period 1976–2005. The green contour in panels (b) and (c) shows the limit of the Negro River Basin.

exceeding 1,000 mm per year over its higher elevations (Figure 1(c)), concentrated mainly during austral winter. This is associated with the south–north displacement of the South Pacific semi-permanent High and the passage of cold fronts (Rivera *et al.* 2018). The topography creates a rainshadow effect that makes the Patagonian steppe a semi-arid region, with annual precipitation below 400 mm.

The Negro river is formed by the Limay and the Neuquén rivers, which are born in the higher elevation of the Andes (Figure 1(a)). The Limay drainage network is complex, characterized by a series of large glacial lakes and a marked vegetation gradient, with rainforests in the west and shrublands in the east in response to the spatial changes in precipitation (Lallement *et al.* 2020). On the other hand, the Neuquén basin lacks natural lakes that regulate its streamflow, with sparse vegetation cover consisting in limited natural forest areas in the west and scattered shrublands in the east (Forni *et al.* 2018). These basins differences result in distinct annual streamflow and annual cycle features among the Limay and Neuquén basins (Berri *et al.* 2019).

2.2. Streamflow observations

Monthly streamflow records from the main rivers in the Comahue region, obtained from the National System of Hydrological Information (https://snih.hidricosargentina.gob.ar/) were used for the validation of simulated streamflow. The selected

gauging stations are located in the Limay, Neuquén, and Negro rivers (Figure 1(a)), and the monthly streamflow records span from 1903 to 2017. Following previous studies (Rivera *et al.* 2018; Lauro *et al.* 2019), these records were subjected to quality control procedures to identify data outliers and periods with spurious sequences with data repetition. Data gaps were identified in the time series of the Limay and Negro rivers. To complete the streamflow records, we applied gap-filling routines based on data from donor stations in the same river or its main tributaries, requesting a coefficient of determination higher than 0.9. Most data gaps were completed by calculating linear regressions between the records from the donor stations and the target stations for infilling. After implementing these procedures, the time series selected for the study retained less than 1% of missing data. Due to data limitations, we used the 1961–1990 reference period for the Limay river and the 1976–2005 period for the Neuquén and Negro rivers.

Limay and Neuquen records are unaffected by river regulation or diversion upstream of the gauging stations (Pichi Picún Leufú Dam became operational after 1999). In contrast, Negro river is expected to exhibit a signal representative of both natural and anthropogenic influences in the streamflow records. It is beyond the scope of this study to separate both components or generate a naturalized streamflow record for Negro river.

2.3. ISIMIP simulations

The ISIMIP project adopted climate and socio-economic input data for multiple impact models used to synthesize expected changes in various sectors considering different levels of global warming (Hempel *et al.* 2013; Warszawski *et al.* 2014). This approach supports adaptation and mitigation decisions requiring regional or global perspectives in the context of facilitating transformations for sustainable development (Rosenzweig *et al.* 2017). Given that the more recent phase of ISIMIP (ISIMIP3b) was under development at the time of conducting this research, we analyzed the impact models from the global water sector belonging to phase 2b of ISIMIP (ISIMIP2b). From the 17 available GHMs, we selected the models with monthly streamflow simulations for at least two emissions scenarios. This condition was satisfied by 10 GHMs, a number that we consider adequate for the evaluation of streamflow variations over the region and is also in line with previous research (Giuntoli *et al.* 2015; Krysanova *et al.* 2017; Veldkamp *et al.* 2017). The 10 GHMs are CLM4.5, H08, JULES-W1, LPJmL, MATSIRO, MPI-HM, ORCHIDEE, ORCHIDEE-DGVM, PCR-GLOBWB, and WaterGAP2-2c (see https://www.isimip.org/impactmodels/ for a summary of the main characteristics). All the GHMs simulate hydrological processes and river routing with a spatial resolution of 0.5° (Hattermann *et al.* 2017). It must be noted that only the WaterGAP2-2c model is calibrated with observed data from 1,319 stations, covering approximately 54% of the global land area (Krysanova *et al.* 2020). These GHMs were driven by climate simulations from four GCMs of the Coupled Model Intercomparison Project Phase 5 (CMIP5) experiment: GFDL-ESM2M, HadGEM2-ES, IPSL-CMSA-LR, and MIROC5 (see Frieler *et al.* 2017 for details). The outputs of these models were subjected to bias correction using the EartH2Observe, WFDEI, and ERA-Interim data Merged and Bias-corrected for ISIMIP (EWEMBI) reanalysis climate product as a basis, resulting in a final spatial resolution of 0.5° latitude by 0.5° longitude. From these models, we analyzed baseline (1976–2005) and future (2021–2050 for the near-term and 2070–2099 for the long-term) monthly temperature, precipitation, and sea level pressure simulations, to account for the main drivers of streamflow variability. The future projections were forced by two of the four available RCPs: the RCP2.6, a low-emission scenario with strong mitigation and in line with a 1.5–2 °C global warming level, and RCP6.0, a business-as-usual greenhouse gas scenario without explicit mitigation measures (Frieler *et al.* 2017).

3. METHODS

3.1. Evaluation of hydrological model performance

A point-to-pixel analysis was performed to compare the time series of streamflow observations to the corresponding hydrological model pixel. We selected the streamflow simulations from the 10 GHMs for the grid points corresponding to the locations of the analyzed stream gauges (Figure 1(a)). To evaluate the performance of ISIMIP2b hydrological models in simulating the amount and variability of the regional streamflow, we used the following comparison statistics: the Pearson correlation coefficient (PCC), the Nash–Sutcliffe efficiency (NSE), the percent bias (PB), the modified Kling–Gupta efficiency (KGE), and the volumetric efficiency (VE). The PCC measures the strength of the linear relationship between the streamflow simulations and the stream gauges observations. The NSE (Nash & Sutcliffe 1970) determines the relative magnitude of the variance of the residuals compared to the variance of the observed streamflow values. The PB measures the average tendency of the simulated streamflow to be larger or smaller than the observed streamflow, where positive values indicate overestimation bias and negative values indicate underestimation bias. The KGE (Gupta *et al.* 2009; Kling *et al.* 2012) is designed as a

more general index that compares the variability of the observed and simulated streamflow values by including information about the correlation between them and their standard deviations, as well as any bias present, expressed by the relation between the mean values. Finally, the VE (Criss & Winston 2008) represents the fractional mismatch of water volume at the proper time. A similar set of metrics was employed by Krysanova *et al.* (2017) for the comparison of simulated and observed streamflow in 12 large river basins worldwide. The optimal value for PPC, NSE, KGE', and VE is 1, while for the PB is 0. Following Duc & Sawada (2023), a NSE of zero is chosen as the boundary between good and bad streamflow simulation, while a KGE higher than −0.41 indicates a good model performance (Knoben *et al.* 2019). For the VE, we used the threshold of 0.33 as a reference for a good streamflow simulation (Ecrepont *et al.* 2019).

3.2. Multi-model ensemble and quantification of future streamflow changes

The performance of the GHMs in the representation of streamflow characteristics was evaluated using the metrics described in Section 3.1. For this purpose, a rating index introduced by Jiang *et al.* (2015) was employed, which provides a comprehensive hierarchical appraisal of model performance. Each model was ranked based on its performance relative to each metric, allocating a rank of 1 for the best-performing model to 10 for the worst. Then, the ranks were aggregated across all the metrics and the three selected rivers. Similar approaches were performed by Balu *et al.* (2023) and Rivera & Arnould (2020) for the selection of the most suitable GCMs. From the rating index, a multi-model ensemble with the best GHMs was selected to quantify the projected changes in streamflow using simulations forced by the RCP2.6 and RCP6.0 scenarios in the near-term (2021–2050) and long-term (2070–2099) future horizons relative to the baseline period of 1976–2005. The mean, median, and range of the change in future streamflow projections were quantified in the results as percentages relative to the baseline period. The uncertainty in streamflow projections was identified from the dispersion of all possible combinations of GHM/GCM, considering also the range of changes from the multi-model ensemble average of the GCMs for each GHM, and for the multi-model ensemble of the GHMs for each GCM. This approach will help identify the main sources of uncertainty in streamflow projections over the study area.

4. RESULTS AND DISCUSSION

4.1. Hydrological model performance of streamflow simulation

To assess the accuracy of the streamflow simulations, we employed a quantitative approach involving the comparison of the observed and simulated hydrological cycles during the baseline period selected for each river. It must be noted that the comparison is made based on the hydrological simulations resulting from the ensemble of the available GCMs. This ensemble was created using a simple arithmetic average.

4.1.1. Limay river

The annual cycle of the Limay river during the period 1961–1990 exhibits a winter (June–July–August) peak attributed to rainfall, with a second peak occurring in late spring (October–November) due to the melt of the winter snowpack from the higher elevations of the Andes (Figure 2). Both peaks are similar in magnitude. The larger variability in monthly streamflow is observed in the months with higher streamflow values. The GHMs generally capture the temporal variability in streamflow, with PPC values ranging from 0.6 to 0.9 (Table 1), in particular, due to a good representation of the winter maximum and the period with minimum streamflows. However, the contribution of snowmelt leading to the second peak is not adequately represented by the GHMs. Models such as CLM45, JULES-W1, ORCHIDEE, ORCHIDEE-DGVM, and PCR-GLOBWB exhibit the largest underestimations in streamflow (Table 1). On the other hand, H08, LPJmL, MPI-HM, and WaterGAP2-2c models tend to overestimate the winter peak, although this difference is compensated during spring months, resulting in modest PB values. Most GHMs underestimate the streamflow values during the period of low streamflows (January–April), with lower variability compared to the observations. These differences resulted in negative values of NSE for most of the models exhibiting the largest PB values, although all the values of KGE' and VE metrics showed a good model performance (Table 1).

4.1.2. Neuquén river

Similar to the Limay river, the annual cycle of the Neuquén river for the period 1976–2005 also shows two distinct streamflow peaks. However, the more significant peak is associated with the snowmelt pulse during late spring, with mean values surpassing 450 m^3 /s in October and November (Figure 3). The largest variability in monthly streamflow is observed between May and December, with a well-defined low-flow period between January and April. All the GHMs underestimate the

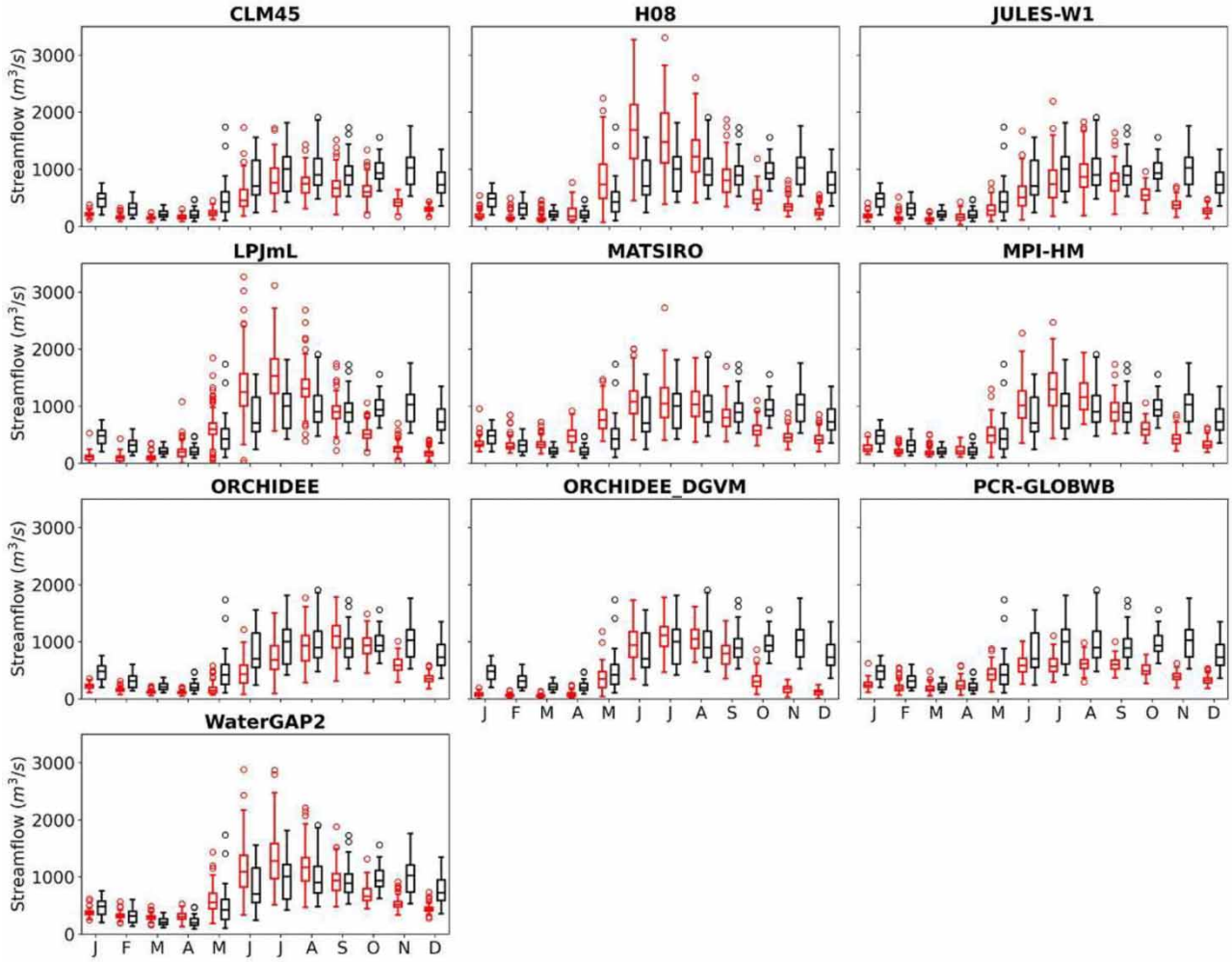

Figure 2 | Boxplot of the mean monthly streamflow simulated by the 10 selected GHMs (red) and the observed streamflow (black) at the Paso Limay station (Limay River) for the period 1961–1990. Each boxplot shows the median and first and third quartiles, while the whiskers extend to the data values that are 1.5 times the interquartile range above or below the quartiles. Extremes are represented by circles.

streamflow values and do not represent the main streamflow peak. This difference between simulated and observed streamflow resulted in lower PCC values in comparison to the results obtained for Limay river, ranging from 0.3 to 0.8. On average, the PB is approximately −50%, with individual GHMs ranging from −17 to −84% (Table 1). The largest underestimations are observed in the simulations from the ORCHIDEE, ORCHIDEE-DGVM, and PCR-GLOBWB models. In particular, the simulations based on ORCHIDEE exhibit a streamflow maximum during spring, while the rest of the models show only a winter maximum. The winter peak is adequately represented by the H08 and LPJmL models but is overestimated in the WaterGAP2-2c simulations (Figure 3). The differences in simulated and observed streamflow resulted in negative values of NSE for ORCHIDEE and ORCHIDEE-DVGM models, and also in a poor performance considering the VE metric (Table 1).

4.1.3. Negro river

As a result of the contributions from both the Limay and Neuquén rivers, the annual cycle of Negro river shows higher streamflows during the winter peak, with mean values of more than 1,000 m^3 /s between June and September (Figure 4). Due to the influences from reservoirs regulating the streamflow over the region, the second maximum during late spring is not as marked as in Limay and Neuquén rivers. Additionally, the low-flow season is attenuated, with streamflow values exceeding 500 m^3 /s. Despite anthropogenic influences in streamflow, the GHMs adequately capture the temporal variability in streamflow, with an average PPC of 0.85, being the highest among the three analyzed rivers (Table 1). The models that

Table 1 | Results from the validation metrics for each river and GHM selected

River	Hydrological model	R	PB	NSE	KGE'	VE
Limay	CLM4.5	0.884	−65.409	−1.589	0.309	0.346
	H08	0.608	7.731	−1.356	0.129	0.459
	JULES-W1	0.832	−31.185	0.187	0.468	0.688
	LPJmL	0.608	−3.140	−1.388	−0.069	0.415
	MATSIRO	0.600	5.348	0.112	0.596	0.635
	MPI-HM	0.744	−1.123	0.217	0.576	0.679
	ORCHIDEE	0.879	−26.421	0.369	0.417	0.695
	ORCHIDEE-DGVM	0.648	−33.026	−0.623	−0.128	0.570
	PCR-GLOBWB	0.881	−66.063	−1.794	0.293	0.339
	WaterGAP2-2c	0.740	7.829	0.176	0.646	0.663
Neuquén	CLM4.5	0.696	−40.291	0.570	0.431	0.575
	H08	0.515	−43.959	0.426	0.121	0.531
	JULES-W1	0.490	−55.751	0.288	0.092	0.442
	LPJmL	0.348	−46.392	0.169	−0.408	0.455
	MATSIRO	0.351	−47.794	0.331	0.115	0.502
	MPI-HM	0.575	−56.795	0.312	0.183	0.432
	ORCHIDEE	0.728	−80.453	−0.134	−0.115	0.195
	ORCHIDEE-DGVM	0.518	−84.076	−0.268	−0.426	0.159
	PCR-GLOBWB	0.751	−61.906	0.285	0.259	0.381
	WaterGAP2-2c	0.418	−17.927	0.301	0.013	0.436
Negro	CLM4.5	0.931	−16.001	−0.797	−0.443	0.752
	H08	0.875	10.227	0.524	0.829	0.871
	JULES-W1	0.851	−24.815	−2.495	−1.064	0.653
	LPJmL	0.765	−3.930	0.591	0.586	0.889
	MATSIRO	0.861	9.662	0.544	0.792	0.877
	MPI-HM	0.914	−3.689	−4.531	−1.539	0.567
	ORCHIDEE	0.751	−35.375	−5.159	−1.975	0.533
	ORCHIDEE-DGVM	0.859	−42.754	−8.083	−3.504	0.455
	PCR-GLOBWB	0.907	−14.869	−0.671	−0.334	0.778
	WaterGAP2-2c	0.815	10.967	0.415	0.589	0.868

exhibit the larger underestimations in streamflow are the same that showed large underestimations for the Limay river, translating this signal to the Negro river, albeit with a lesser magnitude considering the CLM45, JULES-W1, and PCR-GLOBWB models, and with higher underestimations for the ORCHIDEE and ORCHIDEE-DGVM models (Table 1). According to the NSE and the KGE', the GHMs that satisfactorily reproduced the streamflow variability of the Negro river are the H08, LPJmL, MATSIRO, and WaterGAP2-2c. In terms of the VE, all the models showed a good performance.

4.1.4. Regional synthesis and discussion

From the evaluation of the GHMs, a common feature for the selected rivers is that most of the models adequately represented the winter peak in streamflow. Nevertheless, the models fail to reproduce the second peak during late spring, associated with snowmelt contribution, which is particularly important for the Neuquén river. Previous studies showed that this limitation could be explained by a poor estimation of air temperature over the higher elevations of the Andes by the GCMs, a factor that creates a misrepresentation of the snow accumulation during winter and the following contribution as streamflow during spring (Raggio & Saurral 2021). Another striking feature is the capability of the models to reproduce the annual cycle of the Negro river, considering that is highly regulated by large dams located over the Limay and Neuquén rivers (Figure 1). Some of the GHMs include the implementation of dams and reservoirs in the streamflow simulations, for example, the H08, LPJmL, MATSIRO, PCR-GLOBWB, and WaterGAP2-2c, while others include only a routine for irrigation, as the CLM4.5 and the MPI-HM models (see https://www.isimip.org/impactmodels/). Changes in land use and land cover and reservoir operations are responsible for a significant increase in water availability over the lower portion of the Negro basin during both summer and winter (Veldkamp *et al.* 2017). Therefore, this result highlights the need for an adequate representation of streamflow regulations by the GHMs and also

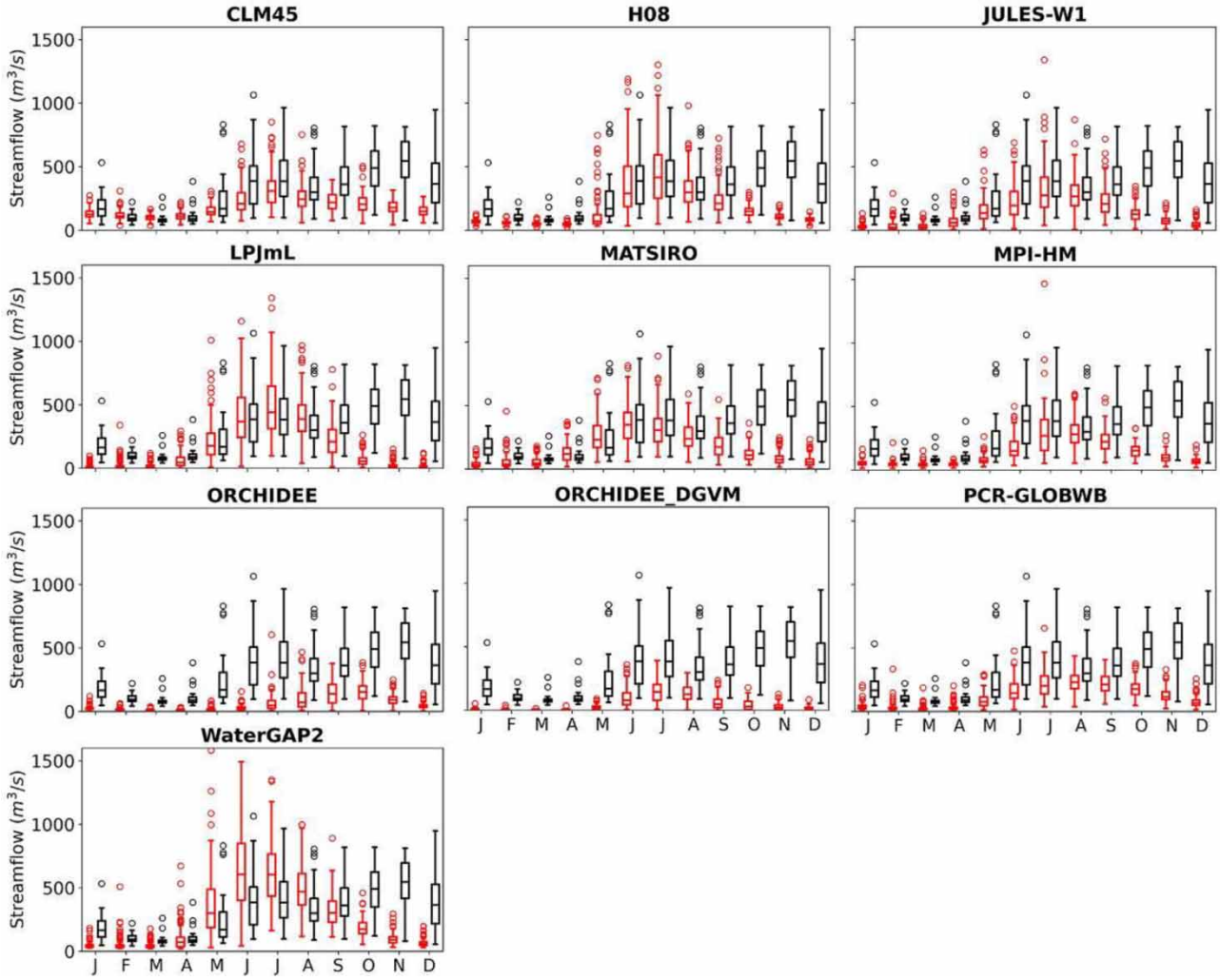

Figure 3 | Boxplot of the mean monthly streamflow simulated by the 10 selected GHMs (red) and the observed streamflow (black) at the Paso de Indios station (Neuquén River) for the period 1976–2005. Each boxplot shows the median and first and third quartiles, while the whiskers extend to the data values that are 1.5 times the interquartile range above or below the quartiles. Extremes are represented by circles.

supports our decision of using observed streamflow over Negro river without removing the water management component.

Considering the rating index, from the initial pool of GHMs, we finally selected the CLM4.5, H08, MATSIRO, MPI-HM, and WaterGAP2-2c for the evaluation of future streamflow conditions over the study area. It must be noted that, among these selected models, H08, MATSIRO, and WaterGAP2-2c incorporate human activities for streamflow regulation, while the models CLM4.5 and MPI-HM include an irrigation scheme in their formulations.

4.2. Future changes in streamflows over northern Patagonia

After selecting the final set of GHMs to represent streamflow in the study area, we assessed the projected changes based on simulations forced by the RCP2.6 and RCP6.0 scenarios in the near-term (2021–2050) and long-term (2070–2099) future horizons relative to the baseline 1976–2005 period. Given the models' challenges in adequately representing the snowmelt peak, we focused on the projection of mean annual streamflow. However, considering that the projected changes can be linked to shifts in the precipitation patterns, particularly the winter rainfall peak, the changes in annual streamflow can be attributed mostly to changes in the winter months.

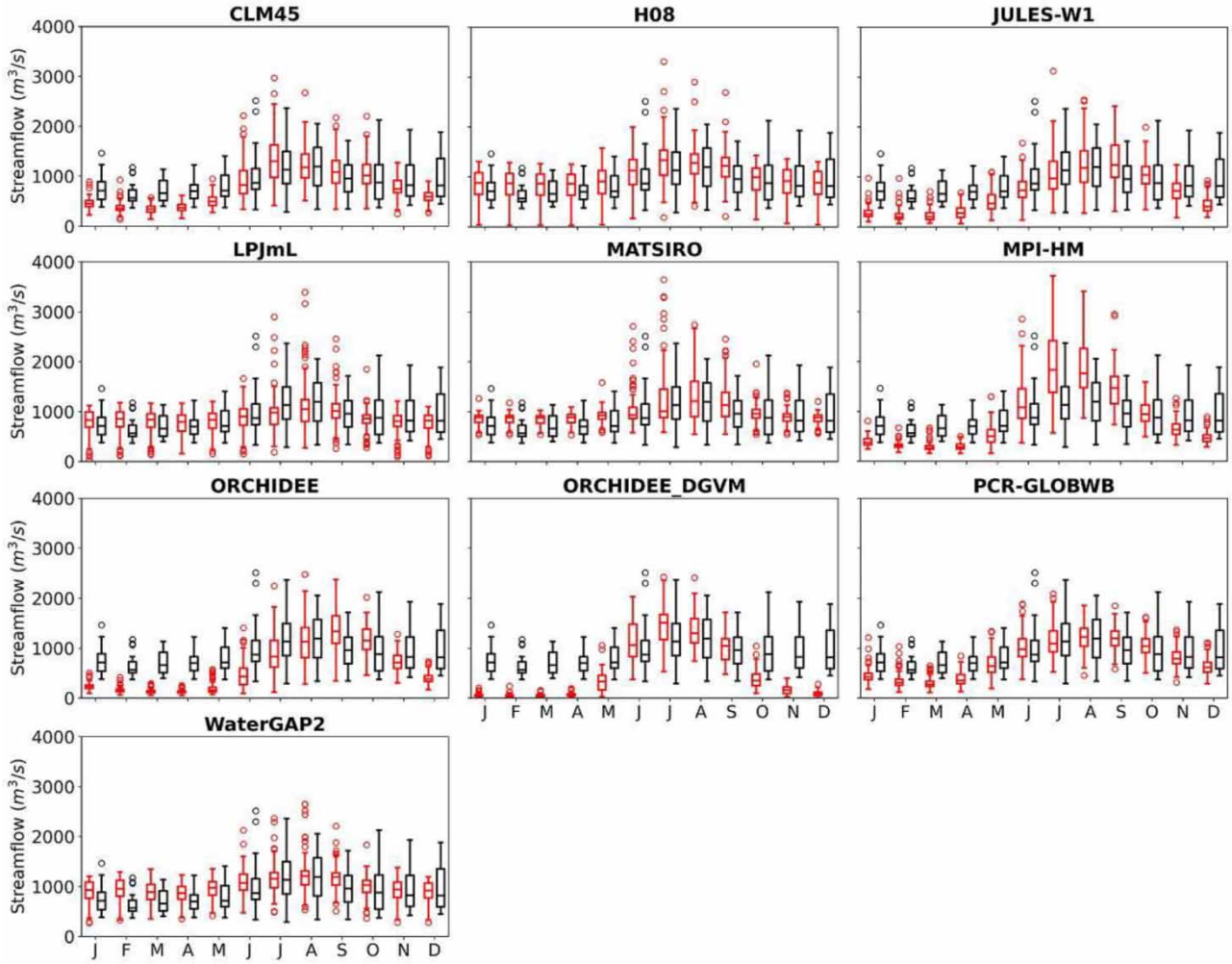

Figure 4 | Boxplot of the mean monthly streamflow simulated by the 10 selected GHMs (red) and the observed streamflow (black) at the Paso Córdoba station (Negro River) for the period 1976–2005. Each boxplot shows the median and first and third quartiles, while the whiskers extend to the data values that are 1.5 times the interquartile range above or below the quartiles. Extremes are represented by circles.

4.2.1. Limay river

Future projections for the Limay river show a decrease in annual streamflow for most of the models and scenarios (Figure 5). On average, the projected reductions range from −10 to −12% for the near-term future under both emissions scenarios, with a larger dispersion for the RCP2.6 scenario. The GHMs forced by the GFDL and MIROC5 models project the highest declines for the 2021–2050 period, especially the CLM4.5 and MPI-HM models, while the HadGEM2 simulations show more moderate decreases (Supplementary material, Tables S1 and S2). Streamflow changes by the end of the century show different responses depending on the emission scenario. Mean reductions of approximately −6% and large dispersion are projected under the RCP2.6 scenario, with average decreases of almost −25% for the RCP6.0 (Figure 5). The hydrologic response to the RCP2.6 scenario leads to small projected increases in annual streamflow by some GHMs forced by the IPSL and MIROC5 climate simulations. However, most simulations project declines in annual streamflow, particularly the GHMs forced by the GFDL simulations (Supplementary material, Table S1). Considering the RCP6.0 scenario, the most relevant streamflow decreases for the 2070–2099 period are projected by the CLM4.5 and MPI-HM hydrological models, with the GFDL simulations leading to reductions of more than −30% in annual streamflow relative to the 1976–2005 baseline (Supplementary material, Table S2).

By evaluating the range of the multi-model projections in Supplementary material (Tables S1 and S2), we can account for the contribution of GHMs and GCMs to the uncertainty in future streamflow projections for the Limay river. We found that

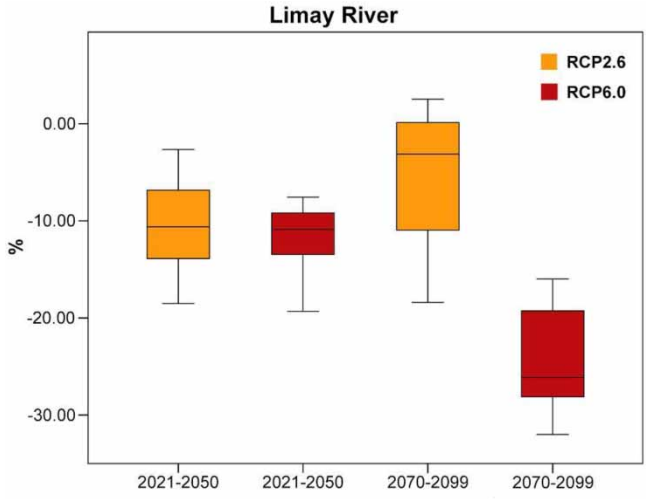

Figure 5 | Boxplot of the projected changes in the annual streamflow of the Limay River for the periods 2021–2050 and 2070–2099, expressed as the percentage of change relative to the 1976–2005 baseline period. The orange (red) boxplots show the projected changes considering the RCP2.6 (RCP6.0) scenario. Each boxplot shows the median and first and third quartiles, while the whiskers extend to the maximum and minimum values of data.

the largest source of uncertainty is associated with the GCMs, a factor that can be linked to the representation of winter precipitation amount and variability. The uncertainty signal is lower for the RCP6.0 scenario, particularly considering the end of the century (Figure 5; Supplementary material, Tables S1 and S2).

4.2.2. Neuquén river

The projected changes in annual streamflow for the Neuquén river show reductions ranging from −10 to −20% for the 2021–2050 period, which could exceed −30% by the end of the century (Figure 6). Mean reductions for the near-term future are similar for both emissions scenarios. Similar to the results obtained for the Limay river, the GHMs that exhibit the largest streamflow reductions are the CLM4.5 and MPI-HM. The highest declines for the 2021–2050 period under the RCP2.6 scenario are projected by the GHMs forced by GFDL and MIROC5 models, while the RCP6.0 scenario exhibits the most important reductions for the GFDL and IPSL models (Supplementary material, Tables S1 and S2). The changes projected for the period 2070–2099 show median values similar to the baseline period considering the RCP2.6 scenario, although with large dispersion and mean reductions of around −5% (Figure 6; Supplementary material, Table S1). Slight streamflow increases are projected for most of the GHMs forced with the HadGEM2 and MIROC5 models, while reductions larger than −20% are depicted by the GFDL model. This result shows that, for this emission scenario, the main source of uncertainty for the quantification of future streamflow at the end of the century is linked to the GCMs and their projected changes in precipitation and temperature over Neuquén river basin. The GHMs forced by the RCP6.0 scenario show average annual streamflow reductions of more than −30% (Figure 6). The most relevant streamflow decreases are projected by the CLM4.5 (–34.8%) and MPI-HM (–42.4%) hydrological models, particularly for the simulations forced with the GFDL and IPSL models (Supplementary material, Table S2). As observed in the Limay river, the uncertainty signal is lower for the RCP6.0 scenario, particularly considering the end of the century (Figure 5; Supplementary material, Tables S1 and S2). In this case, the largest source of uncertainty is associated to the GHMs, a factor that might be linked to the poor representation of the snowmelt processes in this river.

4.2.3. Negro river

In line with the findings described in previous sections, the streamflow response to projected climate change for the Negro river shows a reduction in mean annual streamflow for both the near-term and long-term future periods (Figure 7). The mean projected change for 2021–2050 relative to the baseline period is around −10% for both RCP2.6 and RCP6.0 scenarios, although with higher dispersion for the simulations based on the RCP2.6 scenario. The GHMs projecting the largest streamflow reductions are the CLM4.5 and MPI-HM, particularly when forced with the GFDL model (Supplementary material,

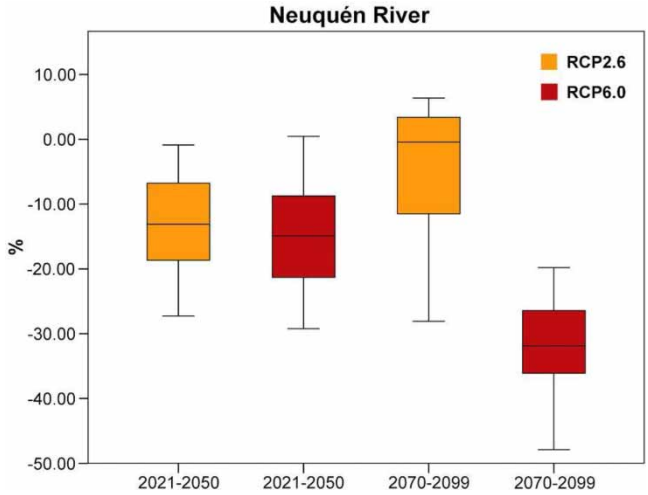

Figure 6 | Boxplot of the projected changes in the annual streamflow of the Neuquén River for the periods 2021–2050 and 2070–2099, expressed as the percentage of change relative to the 1976–2005 baseline period. The orange (red) boxplots show the projected changes considering the RCP2.6 (RCP6.0) scenario. Each boxplot shows the median and first and third quartiles, while the whiskers extend to the maximum and minimum values of data.

Tables S1 and S2). There is a projected recovery in mean annual streamflow for the period 2070–2099 considering the RCP2.6 scenario, with slight increases compared to the baseline period projected for the H08 and WaterGAP2-2c forced with the IPSL and MIROC5 models. However, most simulations show streamflow reductions, with changes close to −20% for the CLM4.5 and MPI-HM models. For the end of the century, the largest streamflow decreases are projected for the RCP6.0 scenario, with mean reductions of almost −30% relative to the baseline period. The most relevant changes are projected with the CLM4.5 and MPI-HM hydrological models, particularly when forced with the GFDL and the IPSL GCMs (Supplementary material, Table S2).

By evaluating the range of the multi-model projections in Supplementary material, Tables S1 and S2, we found that the largest source of uncertainty is associated with the GCMs and, thus, to the representation of winter precipitation amount and variability. The uncertainty signal is lower for the RCP6.0 scenario, particularly considering the end of the century (Figure 7, Supplementary material, Tables S1 and S2).

4.2.4. Regional synthesis and drivers of streamflow changes

The mean annual streamflow of the main rivers in northern Patagonia is projected to decrease over the coming decades, with reductions dependent on the considered emissions scenarios as well as the selected GCM and GHM. The multi-model ensemble shows that the projected reductions for the 2021–2050 period are similar for both emission scenarios, ranging from −10% to −15% for the three analyzed rivers. This result can be linked to the similar changes projected in regional precipitation for the RCP2.6 and RCP6.0 scenarios, ranging from reductions between −5 and −10% in the headwaters of the analyzed rivers (Figure 8). For the near-term future, the hydrological models with the largest projected streamflow reductions are the CLM4.5 and the MPI-HM, particularly when forced with the GFDL and MIROC5 simulations and the RCP2.6 scenario. For the RCP6.0, the GCMs that generate the largest streamflow declines are the GFDL and IPSL. In line with our results, considering a high-emissions scenario, Müller *et al.* (2023) identified a projected decrease in the rivers of the region for the period 2015–2050 of approximately −15%.

The most relevant streamflow reductions are projected for the end of the century, particularly considering the RCP6.0 scenario, with a decrease in mean annual streamflow projected for the multi-model ensemble ranging from −24% for the Limay river to −32% for the Neuquén river. This result aligns with the projected increases in the frequency of days with low flows over northern Patagonia (Giuntoli *et al.* 2015). Considering the results for the Limay river, the projected streamflow reduction is higher than the estimation performed by Seoane & López (2007), which ranged roughly between −11 and −18.5% for the end of the century. Using regional climate models from the CORDEX Project and the InVEST water yield model, Pessacg *et al.* (2020) found a projected decrease in the water yield of Limay river of around −20% for the period 2071–2100. Our

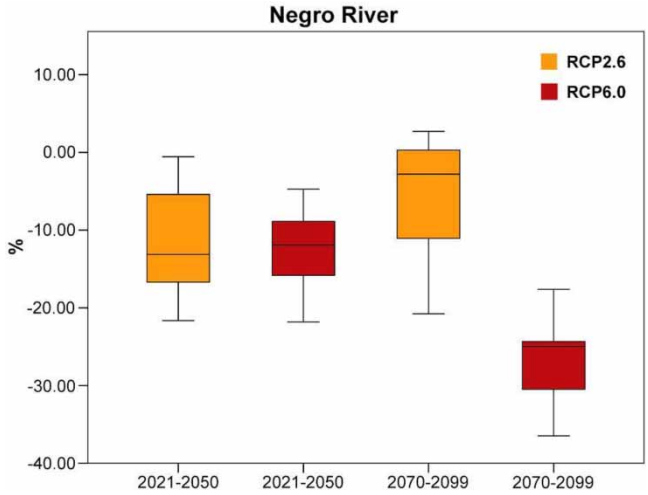

Figure 7 | Boxplot of the projected changes in the annual streamflow of the Negro River for the periods 2021–2050 and 2070–2099, expressed as the percentage of change relative to the 1976–2005 baseline period. The orange (red) boxplots show the projected changes considering the RCP2.6 (RCP6.0) scenario. Each boxplot shows the median and first and third quartiles, while the whiskers extend to the maximum and minimum values of data.

results show that some hydrological simulations exceed −30% of reduction in mean annual streamflow by the end of the century for the RCP6.0 scenario, and an even higher decrease for the streamflow of the Limay river under the RCP8.5 high-emissions scenario was projected with the VIC hydrological model (Raggio & Saurral 2021). The most relevant streamflow reductions are projected by the multi-model ensemble for the Neuquén river, particularly considering the CLM4.5 and MPI-HM hydrological models. Some of the analyzed simulations project a streamflow decline of almost −50% relative to the reference period. In line with our results, previous studies identified a reduction in the available water for irrigation of agricultural areas of the Neuquén river basin (Forni *et al.* 2018). Similar reductions in the mean annual streamflow were projected by the VIC hydrological model under the RCP8.5 scenario (Raggio & Saurral 2021). The streamflow of the Negro river responds to the projected changes in both the Limay and Neuquén rivers, leading to a reduction of approximately −27% in the mean annual streamflow projected by the multi-model ensemble under the RCP6.0 scenario by the end of the century.

By evaluating the range of the multi-model projections, we found that GCMs are mostly responsible for the uncertainty in the streamflow projections, a result that aligns with previous research at global and regional scales (Giuntoli *et al.* 2015; Krysanova *et al.* 2017). The only exception, i.e. GHMs as the main source of uncertainty, was found for the Neuquén river considering the RCP6.0 scenario and the long-term future. This result can be linked to the role of temperature in the snowmelt processes over the basin, as suggested in previous studies (Giuntoli *et al.* 2015; Raggio & Saurral 2021).

The projected decreases in mean annual streamflow can be attributed to several factors, some of which are associated to future precipitation changes in northern Patagonia. Figure 8 shows the projected annual precipitation changes estimated by the multi-model ensemble of GCMs for the 2021–2050 and 2070–2099 periods, forced with the RCP2.6 and RCP6.0 scenarios. For the near-term future, both scenarios exhibit a similar spatial pattern of precipitation change, with projected decreases ranging from −5 to −10% in the headwaters of the main rivers of the region. The projected precipitation decrease is reduced from 0 to −5% for the 2070–2099 period under the RCP2.6 scenario and can be interpreted as the atmospheric response to the mitigation policies included in this scenario (van Vuuren *et al.* 2011). This aligns with the reduced decrease in regional streamflow projected for the same scenario at the end of the century (Figures 5–7). The largest precipitation reductions are projected by the RCP6.0 scenario (Figure 8), particularly over the headwaters of the Nequén river, which exhibits the most relevant projected decreases in streamflow for the 2070–2099 period (Figure 6). This projected trend in precipitation is expected to result in longer and more severe drought events over the region, with serious implications for the development of hydrological droughts (Asadieh & Krakauer 2017; Spinoni *et al.* 2020; Ferreira *et al.* 2023). The projected drying signal for the region can be linked to the projected changes in the mean sea level pressure field across the Southern Hemisphere, particularly during the winter rainy season. For the selected future periods and scenarios, there is a projected increase in the sea level pressure during winter over South America south of 40°S and the South Pacific Ocean, indicating a

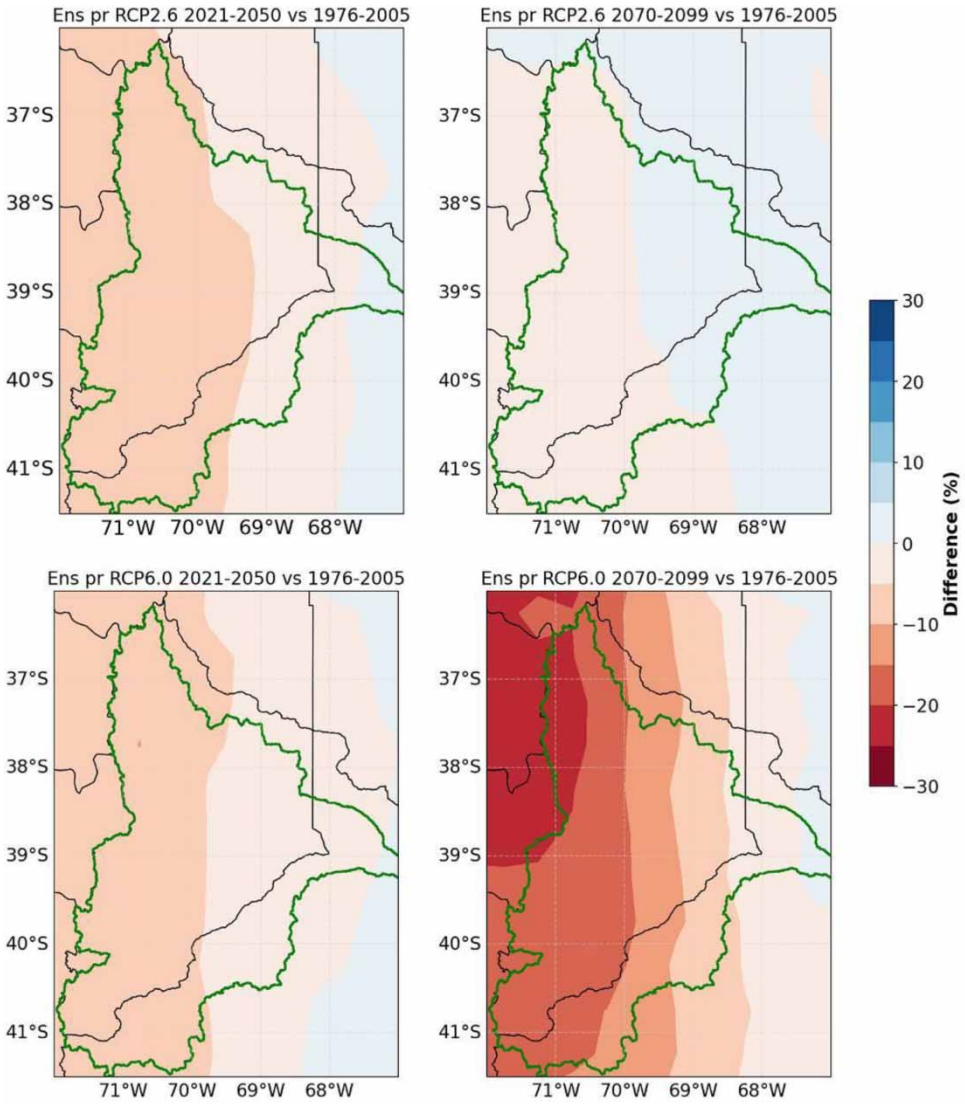

Figure 8 | Projected spatial patterns of annual precipitation changes by the multi-model ensemble of GCMs for 2021–2050 (left panels) and 2070–2099 (right panels) relative to the 1976–2005 period, forced with the RCP2.6 (upper panels) and RCP6.0 (lower panels) scenarios.

strengthening of the semi-permanent anticyclone, particularly during 2070–2099 and considering the RCP6.0 scenario (Supplementary material, Figure S1). Additionally, there is a strengthening of the subpolar low-pressure band, a factor that contributes to an intensification of the southern westerly wind belt, leading to a precipitation decrease over northern Patagonia (Quintana & Aceituno 2011; Rivera & Arnould 2020). The result is also consistent with a poleward expansion of the Hadley Circulation and a positive trend in the Southern Annular Mode, factors that were linked to anthropogenic forcings and thus are dependent on the greenhouse gas emission scenarios (Grise & Davis 2020; Rivera *et al.* 2020; Garreaud *et al.* 2021).

5. CONCLUSIONS

Human-induced climate change is expected to generate a reduction in the streamflow of the main rivers (Limay, Neuquén, and Negro) of the Argentinean portion of northern Patagonia, which account for a significant part of the total hydropower production of the country and allow the irrigation for the main agricultural activities in the region. This was analyzed considering a set of 10 GHMs from the ISIMIP2b dataset, driven by bias-corrected GCMs used to produce future precipitation and temperature projections under the RCP2.6 and RCP6.0 emission scenarios. After a validation procedure, the initial set of GHMs was reduced to five models, adequately representing the winter streamflow peak but not capturing the late-spring

snowmelt pulse. The multi-model ensemble projects a streamflow decrease during the near-term future (2021–2050) of around −10 to −15% compared to the 1976–2005 baseline period, with no dependence upon the selected scenario and river. The uncertainty is given mainly by the different precipitation projections by the GCMs used to drive the GHMs for the streamflow projections, with dispersion in the projected changes of around 20%. Streamflow projections for the long-term future (2070–2099) show divergent responses to the selected scenarios, with a mean reduction of −5 to −6% considering the RCP2.6 scenario but large dispersion in results from individual simulations. This leads to projected streamflow decreases ranging from −20% to slight streamflow increases relative to the reference period. The projected mean reductions using the RCP6.0 are between −20 and −40%, with the Neuquén river showing the most important streamflow decreases. The projected deficit in precipitation in the headwaters of the main rivers in the Comahue region, in response to an increase (decrease) in surface pressure over Patagonia and the South Pacific Ocean (the subpolar low-pressure belt) during winter months, was identified as one of the main drivers of the streamflow decrease over the 21st century.

The results of this study serve as a warning for regional water authorities already facing the challenges of managing reduced water levels for hydropower generation, human consumption, and irrigation for agricultural production. It is important to highlight that this is the first study analyzing such a large and diverse set of streamflow simulations over northern Patagonia. The best GHMs identified in this study can be applied to specific basin-scale research, such as quantifying changes in hydrological extremes. Given that the primary source of uncertainty is associated with the GCMs, it is advisable to consider alternative models to drive the GHMs, particularly those from the latest CMIP6. The adoption of improved bias correction techniques applied to the GCMs has the potential to decrease uncertainty in future projections. Furthermore, it may result in a more accurate representation of snowmelt processes during late spring, a crucial factor limiting the ability to provide precise information regarding the timing and magnitude of the snowmelt pulse, especially over Neuquén river basin.

In light of the projected reduction in surface water availability, the creation of hydrological drought management plans must be developed to ensure water security for local communities and environmental needs, aspects often not considered in regional water management strategies. To achieve this, improved modeling of streamflow processes and a thorough understanding of their future evolution is of paramount importance for providing robust information for decision-makers and water managers.

ACKNOWLEDGEMENTS

This work was supported by the National Agency for Scientific and Technological Promotion (ANPCyT) and the Juan Agustín Maza University (UMaza) under grant PICTO-UUMM-2019-00004, and the National Scientific and Technical Research Council (CONICET) under grant PIBAA 2022–2023 (28720210100485CO).

DATA AVAILABILITY STATEMENT

All relevant data are available from an online repository or repositories.

CONFLICT OF INTEREST

The authors declare there is no conflict.

REFERENCES

Almazroui, M., Ashfaq, M., Islam, M. N., Rashid, I. U., Shahzad, K., Abid, M. A., O'Brien, E., Ismail, M., Reboita, M. S., Sörensson, A. A., Arias, P. A., Alves, L., Tippett, M. K., Saeed, S., Haarsma, R., Doblas-Reyes, F. J., Saeed, F., Kucharski, F., Nadeem, I., Silva-Vidal, Y., Rivera, J. A., Ehsan, M. A., Martínez-Castro, D., Muñoz, A. G., Ali, M. A., Coppola, E. & Sylla, M. B. 2021 Assessment of CMIP6 models performance and projected temperature and precipitation changes over South America. *Earth Systems and Environment* **5**, 155–183. https://doi.org/10.1007/s41748-021-00233-6.

Asadieh, B. & Krakauer, N. Y. 2017 Global change in streamflow extremes under climate change over the 21st century. *Hydrology and Earth System Sciences* **21**, 5863–5874. https://doi.org/10.5194/hess-21-5863-2017.

Balu, A., Ramasamy, S. & Sankar, G. 2023 Assessment of climate change impact on hydrological components of Ponnaiyar river basin, Tamil Nadu using CMIP6 models. *Journal of Water and Climate Change* **14** (3), 730–747. https://doi.org/10.2166/wcc.2023.354.

Berri, G. J., Bianchi, E. & Müller, G. V. 2019 El Niño and La Niña influence on mean river flows of southern South America in the 20th century. *Hydrological Sciences Journal* **64** (8), 900–909. https://doi.org/10.1080/02626667.2019.1609681.

Brendel, A. S., del Barrio, R. A., Mora, F., Orrego León, E. A., Rosales Flores, J. & Campoy, J. A. 2020 Current agro-climatic potential of Patagonia shaped by thermal and hydric patterns. *Theoretical and Applied Climatology* **142**, 855–868. https://doi.org/10.1007/s00704-020-03350-w.

Criss, R. E. & Winston, W. E. 2008 Do Nash values have value? Discussion and alternate proposals. *Hydrological Processes* **22** (14), 2723–2725. https://doi.org/10.1002/hyp.7072.

Dai, A., Qian, T., Trenberth, K. E. & Milliman, J. D. 2009 Changes in continental freshwater discharge from 1948 to 2004. *Journal of Climate* **22** (10), 2773–2792. https://doi.org/10.1175/2008JCLI2592.1.

Duc, L. & Sawada, Y. 2023 A signal-processing-based interpretation of the Nash–Sutcliffe efficiency. *Hydrology and Earth System Sciences* **27** (9), 1827–1839. https://doi.org/10.5194/hess-27-1827-2023.

Ecrepont, S., Cudennec, C., Anctil, F. & Jaffrézic, A. 2019 PUB in Québec: A robust geomorphology-based deconvolution-reconvolution framework for the spatial transposition of hydrographs. *Journal of Hydrology* **570**, 378–392. https://doi.org/10.1016/j.jhydrol.2018.12.052.

Ferreira, G. W. d. S., Reboita, M. S., Ribeiro, J. G. M. & de Souza, C. A. 2023 Assessment of precipitation and hydrological droughts in South America through statistically downscaled CMIP6 projections. *Climate* **11** (8), 166. https://doi.org/10.3390/cli11080166.

Forni, L., Escobar, M., Cello, P., Marizza, M., Nadal, G., Girardin, L., Losano, F., Bucciarelli, L., Young, C. & Purkey, D. 2018 Navigating the water-energy governance landscape and climate change adaptation strategies in the Northern Patagonia Region of Argentina. *Water* **10** (6), 794. https://doi.org/10.3390/w10060794.

Frieler, K., Lange, S., Piontek, F., Reyer, C. P. O., Schewe, J., Warszawski, L., Zhao, F., Chini, L., Denvil, S., Emanuel, K., Geiger, T., Halladay, K., Hurtt, G., Mengel, M., Murakami, D., Ostberg, S., Popp, A., Riva, R., Stevanovic, M., Suzuki, T., Volkholz, J., Burke, E., Ciais, P., Ebi, K., Eddy, T. D., Elliott, J., Galbraith, E., Gosling, S. N., Hattermann, F., Hickler, T., Hinkel, J., Hof, C., Huber, V., Jägermeyr, J., Krysanova, V., Marcé, R., Müller Schmied, H., Mouratiadou, I., Pierson, D., Tittensor, D. P., Vautard, R., van Vliet, M., Biber, M. F., Betts, R. A., Bodirsky, B. L., Deryng, D., Frolking, S., Jones, C. D., Lotze, H. K. & Lotze-Campen, H. *et al.* 2017 Assessing the impacts of 1.5 °C global warming – simulation protocol of the Inter-Sectoral Impact Model Intercomparison Project (ISIMIP2b). *Geoscientific Model Development* **10** (12), 4321–4345. https://doi.org/10.5194/gmd-10-4321-2017.

Garreaud, R. D., Clem, K. & Veloso, J. V. 2021 The south pacific pressure trend dipole and the southern blob. *Journal of Climate* **34** (18), 7661–7676. https://doi.org/10.1175/JCLI-D-20-0886.1.

Giuntoli, I., Vidal, J.-P., Prudhomme, C. & Hannah, D. M. 2015 Future hydrological extremes: The uncertainty from multiple global climate and global hydrological models. *Earth System Dynamics* **6**, 267–285. https://doi.org/10.5194/esd-6-267-2015.

González, M. H., Skansi, M. M. & Losano, F. 2010 A statistical study of seasonal winter rainfall prediction in the Comahue region (Argentina). *Atmósfera* **23** (3), 277–294.

González, M. H., Rolla, A. L. & Sanchez, M. V. 2023 Seasonal probabilistic precipitation prediction in Comahue region (Argentina) using statistical techniques. *Theoretical and Applied Climatology* **151**, 1483–1495. https://doi.org/10.1007/s00704-022-04324-w.

Gosling, S. N., Zaherpour, J., Mount, N. J., Hattermann, F. F., Dankers, R., Arheimer, B., Breuer, L., Ding, J., Haddeland, I., Kumar, R., Kundu, D., Liu, J., van Griensven, A., Veldkamp, T. I. E., Vetter, T., Wang, X. & Zhang, X. 2017 A comparison of changes in river runoff from multiple global and catchment-scale hydrological models under global warming scenarios of 1 °C, 2 °C and 3 °C. *Climatic Change* **141**, 577–595. https://doi.org/10.1007/s10584-016-1773-3.

Grise, K. M. & Davis, S. M. 2020 Hadley cell expansion in CMIP6 models. *Atmospheric Chemistry and Physics* **20** (9), 5249–5268. https://doi.org/10.5194/acp-20-5249-2020.

Gulev, S. K., Thorne, P. W., Ahn, J., Dentener, F. J., Domingues, C. M., Gerland, S., Gong, D., Kaufman, D. S., Nnamchi, H. C., Quaas, J., Rivera, J. A., Sathyendranath, S., Smith, S. L., Trewin, B., von Schuckmann, K., Vose, R. S., 2021 Changing State of the Climate System. In: *Climate Change 2021: The Physical Science Basis. Contribution of Working Group I to the Sixth Assessment Report of the Intergovernmental Panel on Climate Change* (Masson-Delmotte, V., Zhai, P., Pirani, A., Connors, S. L., Péan, C., Berger, S., Caud, N., Chen, Y., Goldfarb, L., Gomis, M. I., Huang, M., Leitzell, K., Lonnoy, E., Matthews, J. B. R., Maycock, T. K., Waterfield, T., Yelekçi, O., Yu, R. & Zhou, B., eds). Cambridge University Press, Cambridge, United Kingdom andNew York, NY, USA, pp. 287–422. https://doi.org/10.1017/9781009157896.004..

Gupta, H. V., Kling, H., Yilmaz, K. K. & Martinez, G. F. 2009 Decomposition of the mean squared error and NSE performance criteria: Implications for improving hydrological modelling. *Journal of Hydrology* **377** (1–2), 80–91. https://doi.org/10.1016/j.jhydrol.2009.08.003.

Hattermann, F. F., Krysanova, V., Gosling, S. N., Dankers, R., Daggupati, P., Donnelly, C., Flörke, M. & Huang, S. 2017 Cross-scale intercomparison of climate change impacts simulated by regional and global hydrological models in eleven large river basins. *Climatic Change* **141**, 561–576. https://doi.org/10.1007/s10584-016-1829-4.

Hempel, S., Frieler, K., Warzawski, L., Schewe, J. & Piontek, F. 2013 A trend-preserving bias correction – the ISI-MIP approach. *Earth System Dynamics* **4** (2), 219–236. https://doi.org/10.5194/esd-4-219-2013.

Hock, R., Bliss, A., Marzeion, B., Giesen, R., Hirabayashi, Y., Huss, M., Radic, V. & Slangen, A. 2019 GlacierMIP – A model intercomparison of global-scale glacier mass-balance models and projections. *Journal of Glaciology* **65** (251), 453–467. https://doi.org/10.1017/jog.2019.22.

Huss, M., Bookhagen, B., Huggel, C., Jacobsen, D., Bradley, R. S., Clague, J. J., Vuille, M., Buytaert, W., Cayan, D. R., Greenwood, G., Mark, B. G., Milner, A. M., Weingartner, R. & Winder, M. 2017 Toward mountains without permanent snow and ice. *Earth's Future* **5** (5), 418–435. https://doi.org/10.1002/2016EF000514.

Jiang, Z., Li, W., Xu, J. & Li, L. 2015 Extreme precipitation indices over China in CMIP5 models. Part I: Model evaluation. *Journal of Climate* **28** (21), 8603–8619. https://doi.org/10.1175/JCLI-D-15-0099.1.

Ju, J., Wu, C., Li, J., Yeh, P. J.-F. & Hu, B. X. 2023 Global evaluation of model agreement and uncertainty in terrestrial water storage simulations from ISIMIP 2b framework. *Journal of Hydrology* **617**, 129137. https://doi.org/10.1016/j.jhydrol.2023.129137.

Kling, H., Fuchs, M. & Paulin, M. 2012 Runoff conditions in the upper Danube basin under an ensemble of climate change scenarios. *Journal of Hydrology* **424–425**, 264–277. https://doi.org/10.1016/j.jhydrol.2012.01.011.

Knoben, W. J. M., Freer, J. E. & Woods, R. A. 2019 Technical note: Inherent benchmark or not? Comparing Nash–Sutcliffe and Kling–Gupta efficiency scores. *Hydrology and Earth System Sciences* **23** (10), 4323–4331. https://doi.org/10.5194/hess-23-4323-2019.

Krysanova, V., Vetter, T., Eisner, S., Huang, S., Pechlivanidis, I., Strauch, M., Gelfan, A., Kumar, R., Aich, V., Arheimer, B., Chamorro, A., van Griensven, A., Kundu, D., Lobanova, A., Mishra, V., Plötner, S., Reinhardt, J., Seidou, O., Wang, X., Wortmann, M., Zeng, X. & Hattermann, F. F. 2017 Intercomparison of regional-scale hydrological models and climate change impacts projected for 12 large river basins worldwide – a synthesis. *Environmental Research Letters* **12** (10), 105002. https://doi.org/10.1088/1748-9326/aa8359.

Krysanova, V., Donnelly, C., Gelfan, A., Gerten, D., Arheimer, B., Hattermann, F. & Kundzewicz, Z. W. 2018 How the performance of hydrological models relates to credibility of projections under climate change. *Hydrological Sciences Journal* **63** (5), 696–720. https://doi.org/10.1080/02626667.2018.1446214.

Krysanova, V., Zaherpour, J., Didovets, I., Gosling, S. N., Gerten, D., Hanasaki, N., Müller Schmied, H., Pokhrel, Y., Satoh, Y., Tang, Q. & Wada, Y. 2020 How evaluation of global hydrological models can help to improve credibility of river discharge projections under climate change. *Climatic Change* **163**, 1353–1377. https://doi.org/10.1007/s10584-020-02840-0.

Lallement, M. E., Rechencq, M., Fernández, M. V., Zattara, E., Sosnovsky, A., Vigliano, P., Garibotti, G., Alonso, M. F., Lippolt, G. & Macchi, P. J. 2020 Landscape factors modulating patterns of salmonid distribution during summer in north Patagonian rivers. *Journal of Fish Biology* **97**, 753–762. https://doi.org/10.1111/jfb.14431.

Lauro, C., Vich, A. I. & Moreiras, S. M. 2019 Streamflow variability and its relationship with climate indices in western rivers of Argentina. *Hydrological Sciences Journal* **64** (5), 607–619. https://doi.org/10.1080/02626667.2019.1594820.

Miller, O. L., Putman, A. L., Alder, J., Miller, M., Jones, D. K. & Wise, D. R. 2021 Changing climate drives future streamflow declines and challenges in meeting water demand across the southwestern United States. *Journal of Hydrology X* **11**, 100074. https://doi.org/10.1016/j.hydroa.2021.100074.

Mindlin, J., Shepherd, T. G., Vera, C. S., Osman, M., Zappa, G., Lee, R. W. & Hodges, K. I. 2020 Storyline description of Southern Hemisphere midlatitude circulation and precipitation response to greenhouse gas forcing. *Climate Dynamics* **54**, 4399–4421. https://doi.org/10.1007/s00382-020-05234-1.

Müller, O. V., McGuire, P., Vidale, P. L. & Hawkins, E. 2023 River flow in the near future: A global perspective in the context of a high-emission climate change scenario. *EGUsphere*. https://doi.org/10.5194/egusphere-2023-1281.

Nash, J. E. & Sutcliffe, J. V. 1970 River flow forecasting through conceptual models part I – A discussion of principles. *Journal of Hydrology* **10** (3), 282–290. https://doi.org/10.1016/0022-1694(70)90255-6.

Pessacg, N., Flaherty, S., Solman, S. & Pascual, M. 2020 Climate change in northern Patagonia: Critical decrease in water resources. *Theoretical and Applied Climatology* **140**, 807–822. https://doi.org/10.1007/s00704-020-03104-8.

Raggio, G. A. & Saurral, R. I. 2021 Probable intensificación de las condiciones de déficit hídrico sobre la región del Comahue ante diversos escenarios de cambio climático. *Meteorologica* **46** (1), e004. https://doi.org/10.24215/1850468Xe004.

Rivera, J. A. & Arnould, G. 2020 Evaluation of the ability of CMIP6 models to simulate precipitation over Southwestern South America: Climatic features and long-term trends (1901–2014). *Atmospheric Research* **241**, 104953. https://doi.org/10.1016/j.atmosres.2020.104953.

Rivera, J. A., Araneo, D. C., Penalba, O. C. & Villalba, R. 2018 Regional aspects of streamflow droughts in the Andean rivers of Patagonia, Argentina. Links with large-scale climatic oscillations. *Hydrology Research* **49** (1), 134–149. https://doi.org/10.2166/nh.2017.207.

Rivera, J. A., Naranjo Tamayo, E. & Viale, M. 2020 Water resources change in Central-Western Argentina under the Paris Agreement warming targets. *Frontiers in Climate* **2**, 587126. https://doi.org/10.3389/fclim.2020.587126.

Romero, P. E., González, M. H., Rolla, A. L. & Losano, F. 2020 Forecasting annual precipitation to improve the operation of dams in the Comahue region, Argentina. *Hydrological Sciences Journal* **65** (11), 1974–1983. https://doi.org/10.1080/02626667.2020.1786570.

Rosenzweig, C., Arnell, N. W., Ebi, K. L., Lotze-Campen, H., Raes, F., Rapley, C., Smith, M. S., Cramer, W., Frieler, K., Reyer, C. P. O., Schewe, J., Van Vuuren, D. & Warszawski, L. 2017 Assessing inter-sectoral climate change risks: The role of ISIMIP. *Environmental Research Letters* **12**, 1. https://doi.org/10.1088/1748-9326/12/1/010301.

Seoane, R. & López, P. 2007 Assessing the effects of climate change on the hydrological regime of the Limay River basin. *GeoJournal* **70**, 251–256. https://doi.org/10.1007/s10708-008-9138-8.

Shannon, S., Smith, R., Wiltshire, A., Payne, T., Huss, M., Betts, R., Caesar, J., Koutroulis, A., Jones, D. & Harrison, S. 2019 Global glacier volume projections under high-end climate change scenarios. *The Cryosphere* **13** (1), 325–350. https://doi.org/10.5194/tc-13-325-2019.

Spinoni, J., Barbosa, P., Bucchignani, E., Cassano, J., Cavazos, T., Christensen, J. H., Christensen, O. B., Coppola, E., Evans, J., Geyer, B., Giorgi, F., Hadjinicolaou, P., Jacob, D., Katzfey, J., Koenigk, T., Laprise, R., Lennard, C. H., Levent Kurnaz, M., Li, D., Llopart, M., McCormick, N., Naumann, G., Nikulin, G., Ozturk, T., Panitz, H.-J., Porfirio da Rocha, R., Rockel, B., Solman, S. A., Syktus, J., Tangang, F., Teichmann, C., Vautard, R., Vogt, J. V., Winger, K., Zittis, G. & Dosio, A. 2020 Future global meteorological drought hotspots. A study based on CORDEX data. *Journal of Climate* **33** (9), 3635–3661. https://doi.org/10.1175/JCLI-D-19-0084.1.

van Vuuren, D. P., Stehfest, E., den Elzen, M. G. J., Kram, T., van Vliet, J., Deetman, S., Isaac, M., Goldewijk, K. K., Hof, A., Mendoza Beltran, A., Oostenrijk, R. & van Ruijven, B. 2011 RCP2.6: Exploring the possibility to keep global mean temperature increase below 2 °C. *Climatic Change* **109**, 95. https://doi.org/10.1007/s10584-011-0152-3.

Veldkamp, T. I. E., Wada, Y., Aerts, J. C. J. H., Döll, P., Gosling, S. N., Liu, J., Masaki, Y., Oki, T., Ostberg, S., Pokhrel, Y., Satoh, Y., Kim, H. & Ward, P. J. 2017 Water scarcity hotspots travel downstream due to human interventions in the 20th and 21st century. *Nature Communications* **8**, 15697. https://doi.org/10.1038/ncomms15697.

Vich, A. I. J., Norte, F. A. & Lauro, C. 2014 Análisis regional de frecuencias de caudales de ríos pertenecientes a cuencas con nacientes en la Cordillera de los Andes. *Meteorologica* **39** (1), 3–26.

Villamayor, J., Khodri, M., Villalba, R. & Daux, V. 2021 Causes of the long-term variability of southwestern South America precipitation in the IPSL-CM6A-LR model. *Climate Dynamics* **57**, 2391–2414. https://doi.org/10.1007/s00382-021-05811-y.

Warszawski, L., Frieler, K., Huber, V., Piontek, F., Serdeczny, O. & Schewe, J. 2014 The inter-sectoral impact model intercomparison project (ISI-MIP): Project framework. *Proceedings of the National Academy of Sciences of the United States of America* **111** (9), 3228–3232. https://doi.org/10.1073/pnas.1312330110.

Zaherpour, J., Gosling, S. N., Mount, N., Müller Schmied, H., Veldkamp, T. I. E., Dankers, R., Eisner, S., Gerten, D., Gudmundsson, L. & Haddeland, I. 2018 Worldwide evaluation of mean and extreme runoff from six global-scale hydrological models that account for human impacts. *Environmental Research Letters* **13** (6), 065015. https://doi.org/10.1088/1748-9326/aac547.

Zhang, W., Liang, W., Tian, L. & Zhao, X. 2023 Climatic and different human influences on annual and seasonal streamflow with considering the soil water storage change in the middle reaches of the Yellow River basin, China. *Journal of Hydrology* **619**, 129298. https://doi.org/10.1016/j.jhydrol.2023.129298.

First received 3 September 2023; accepted in revised form 22 March 2024. Available online 2 April 2024